EFDA–JET–PR(06)03

H. Leggate, J.G. Cordey, J. Snipes, P.J. Lomas, D.C. McDonald,
G. Maddison, C.C. Petty, I.Voitsekhovitch
and JET EFDA contributors

The Significance of the Dimensionless Collisionality and the Greenwald Fraction in the Scaling of Confinement

The Significance of the Dimensionless Collisionality and the Greenwald Fraction in the Scaling of Confinement

H. Leggate[1], J.G. Cordey[1], J. Snipes[3], P.J. Lomas[1], D.C. McDonald[1], G. Maddison[1],C.C. Petty2, I. Voitsekhovitch[1] and JET EFDA contributors*

[1] EURATOM/UKAEA Fusion Association, Culham Science Centre, Abingdon, OX14 3DB, UK
[2] General Atomics, PO Box 85608, San Diego,CA 92186, USA
[3] Plasma Science and Fusion Center, MIT, Cambridge, MA 02139, USA
** See annex of J. Pamela et al, "Overview of JET Results ", (Proc. 20th IAEA Fusion Energy Conference, Vilamoura, Portugal (2004)).*

Preprint of Paper to be submitted for publication in
Nuclear Fusion

ABSTRACT.

Although for a fully ionised plasma the main dimensionless parameters which control the plasma confinement are the normalised Larmor radius ρ*, plasma β, and normalised collisionality ν*, some experimental results have indicated that the density normalised to the Greenwald density limit F_{gr} (≡ $n\pi a^2/I$) may be a relevant parameter. To resolve this question identity experiments have been completed on tokamaks of different size in which first ρ*, β, ν* and then ρ*, β, F_{gr} are matched. The dimensionless confinement times $\omega_c\tau_E$ on each tokamak are then compared. Initial experiments on JET and DIII-D indicated that ρ*, β, and ν* were the key parameters, however one could not exclude ρ*, β, and F_{gr} within the errors of the measurement. The reason for this is that the difference in ν* at fixed ρ*, β, F_{gr} and F_{gr} at fixed ρ*, β, ν* scales with minor radius a and since the size ratio of JET to DIII-D is only a factor of 1.6 the differences in the unmatched parameter and hence any effect on τ_E is small. This paper describes similarity experiments performed on JET and Alcator-CMOD, which have a size ratio of factor 4. The ρ*, β, ν* and ρ*, β, F_{gr} matches were achieved by performing an ELMy H-mode ν* scan on JET in the Alcator-CMOD geometry with ρ*, β, and q at the same value as an Alcator-CMOD pulse. The scan included separate pulses where both ν* and F_{gr} were matched in both machines. The ratio of the normalised global confinement for the two machines ($\omega_c\tau_E$ (JET)/$\omega_c\tau_E$ (CMOD)) for the ρ*, β, ν* match was 1.08, for the ρ*, β, F_{gr} match the ratio was 2.65. This indicates that ν* is the more relevant parameter for confinement scaling.

1. INTRODUCTION

Assuming that energy confinement is dominated by the physics of fully ionised plasmas, it has been shown, theoretically, that the normalised energy confinement time ($\omega_c\tau_E \propto B_T\tau_E$) can be expressed in terms of the three dimensionless parameters ρ^* ($\propto m_i^{0.5}\, T_i^{0.5}/aB_T$), ν^* ($\propto Z_{eff} n_e\, aq/T_e^{\,2}$) and β ($\propto p/B^2_T$) [1, 2] where *mi* is the ion mass, T_e and T_i are the electron and ion temperatures, n_e is the electron density, R is the major radius, a is the minor radius, B_T is the toroidal magnetic field, ω_c is the ion cyclotron frequency and τ_E is the energy confinement time, $B_T\tau_E$ will be used in preference to $\omega_c\tau_E$ in the rest of this paper. This would imply that tokamaks of different physical size will have the same normalised energy confinement when these parameters are matched along with with the same plasma geometry and safety factor ($q \propto aB_T/RB_P$), where *BP* is the poloidal magnetic field. Such experiments have been performed between JET and DIII-D [3, 4], JET and ASDEX-Upgrade [5], and JET and Alcator-CMOD [6], and all indicate that this is indeed the case.

Another important dimensionless plasma parameter relevant to tokamak physics is the Greenwald fraction F_{gr} ($\equiv n/n_{gr}$), where n_{gr} is the empirically derived Greenwald density limit[7] given by

$$n_{gr}\,(10^{20}\ \mathrm{m}^{-3}) = \frac{I_p(\mathrm{MA})}{\pi a^2(m)} \qquad (1)$$

where a is the plasma minor radius and I_p is the plasma current. F_{gr} cannot be expressed in terms of

ρ^*, β, ν^* alone[8], indicating that it is not a parameter of a fully ionised plasma. Instead, F_{gr} can be viewed as representing atomic physics as it may be written

$$F_{gr} = \frac{n}{n_{gr}} \propto \frac{q\beta}{\epsilon\rho^*}\left(\frac{\xi}{T_e}\right)^{1/2} \tag{2}$$

where 2 is the inverse aspect ratio, T_e is the electron temperature and ξ_a is the atomic unit of energy given by,

$$\xi_a = \frac{m_e e^4}{h^2} \approx 27eV \tag{3}$$

where m_e is the electron mass and e is the electron charge. The inclusion of the absolute temperature as an identity parameter has been shown to represent atomic physics [9, 10, 11]. F_{gr} is clearly important in determining density limits for radiative collapse in tokamak plasmas [8]. However, there is evidence to suggest that F_{gr} may also be a relevant parameter for confinement. Experiments performed on JET [12] have shown that confinement normalised to the IPB98(y,2) scaling (H98) decreases as n_{gr} is approached over the range $0.5 < F_{gr} < 0.9$. Similar results have also been obtained on ASDEX-Upgrade [13], DIIID [14] and JT-60 [15]. As a result of these experiments the relevance of plasma scenarios to a next step device such as ITER is often demonstrated by showing that they can achieve good confinement for a given F_{gr} [16, 17, 18]. Implicit in such analyses is the assumption that confinement depends on F_{gr}. Such a dependency would imply that contrary to earlier indications, atomic physics affects plasma confinement.

To test experimentally if confinement depends on F_{gr}, the confinement of plasma with matched ρ^*, β, ν^* but differing F_{gr} can be compared. For matched ρ^*, β, ν^*, $F_{gr} \propto a^{1/4}$, meaning that such matches must be made between machines of different sizes. By performing a similar match of ρ^*, β, and F_{gr} at differing ν^*, the dependency of confinement on F_{gr} may be compared with its dependency on ν^*.

To test the hypothesis that Fgr is a valid scaling parameter identity discharges matching ρ^*, β, F_{gr} were performed on DIII-D and JET [19]. The scaled global energy confinement on the two machines was found to differ by about 20%. Previous similarity experiments matching ρ^*, β, ν^*, [4, 3] show agreement in global and local confinement to within 5%, suggesting that ν^* is the more appropriate parameter. This suggests that edge atomic physics and other effects do not play a dominant role in energy confinement and that the degradation of normalised confinement as n_{gr} is approached is due to a degradation in ν^*. However, the small difference in ν^* for the F_{gr} match, which is a consequence of the similar sizes of JET and DIII-D ($a_{JET}/a_{DIII\text{-}D} \approx 1.5$) was too small for a conclusive result. The Alcator-CMOD tokamak has a minor radius of 0.22m, giving a size ratio $a_{JET}/a_{CMOD} \approx 4$. It is also possible to achieve matched geometries between JET and Alcator-CMOD, so experiments matching first F_{gr} and then ν^* were lQrformed on the two machines.

The rest of this paper is structured as follows. Section 2 describes the experimental conditions

for the ρ^*, β, F_{gr} and ρ^*, β, ν^* matches. Section 3 describes the experimental results and section 4 presents a summary of the work and the conclusions drawn from it.

2. EXPERIMENTAL SET-UP

Databases of JET and Alcator-CMOD shots were compared in order to find a configuration suitable for both machines. Pulses were then run on Alcator-CMOD and pulse 1001018013 at time 1.26s was chosen as the most suitable candidate for matches in ν^* and F_{gr}. A collisionality scan was then performed on JET with the MarkIIGB-SRP divertor at fixed ρ^*, β, q, and plasma geometry (see figure 1), all matching the chosen CMOD pulse. The dimensionless parameters were matched by tuning ICRH power and gas puffing and using the relations $\beta \propto W_{th}/aI^2$, $\rho^* \propto (W_{th}/na^3)^{1/2} I^{-1}$ and $\nu^* \propto n^3 a^7 / W_{th}^2$, where W_{th} is the thermal stored energy. W_{th} was calculated using the measured *WDIA* and subtracting the fast particle contribution calculated by the PION code [20]. ICRH heating was used in all shots. All discharges were single null, steady state ELMy H-modes without significant NTM or MARFE activity [21].

Electron density on JET was measured with an 8 channel interferometry system [22] and a LIDAR Thomson scattering system [23], from which electron temperature measurements were also taken. Charge exchange spectroscopy [24] was not available as the discharges were heated by ICRH. The ion temperature was therefore taken to be equal to the electron temperature. The kinetic measurements were found to agree with the measured stored energy to within the measurement uncertainties of 15%. Z_{eff} was calculated using the visible bremsstrahlung radiation. Equilibria and q profiles were initially reconstructed using the EFIT code [25] based on data from magnetic coils.

3. EXPERIMENTAL RESULTS

The global results for the three discharges are given in table 1. The Greenwald match was achieved at the lowest end of the JET ν^* scan with F_{gr} matched to within 2%. The ν^* match was achieved at lower field and current and agrees to within 1%. The best matches were found at 31.38s during shot 62663 for the ν^* match and 34.68s during shot 62657 for the Greenwald match. Type III ELMs are observed with periodic transitions into ELM-free H-mode and occasionally L-mode (see figures 2, 3 and 4), both matches were made during type III periods to match the CMOD ELM regime. Sawteeth were observed during both JET discharges. The estimated random errors on the dimensionless parameters for all discharges are given in table 1. The scaling of τ_E is relatively unaffected by systematic errors, which are not included here. The two JET shots are matched to the CMOD shot within the quoted errors in all the relevant dimensionless parameters. The normalised global confinement is the same to within 1 standard deviation for the JET ν^* matched shot and the CMOD shot. For the JET Greenwald fraction matched shot the normalised global confinement differs from the CMOD value by more than a factor two. This difference is equivalent to 5 standard deviations and supports the assertion that τ_E is the more relevant dimensionless parameter [19]. This can be clearly seen in figures 5(a) and 5(b), which show the dimensionless confinement time

$B\tau_E$ against ν^* and $B\tau_E$ against the Greenwald fraction F_{gr}. Small differences in ρ^* across the scan (see table 1) can affect this result. This can be assessed by normalising $B\tau_E$ to $(\rho^*/\rho^*_{CMOD})^{-2.7}$, where $B\tau_E \propto \rho^{*-2.7}$ is the ρ^* scaling from IPB98(y,2). The result of this normalisation can be seen in figures 6(a) and 6(b) and shows that the differences in ρ^* are not significant.

3.1. LOCAL TRANSPORT

The local values of the dimensionless parameters give a more detailed view of the differences in confinement. As neutral beam injection was not used, no charge exchange data was available. T_i was therefore taken to be equal to T_e and the Z_{eff} profile was assumed to be flat. Transport analysis was performed using the TRANSP code [26, 27]. The q profiles were calculated internally by TRANSP. Electron density and temperature profiles were smoothed over a 1s time window. The matched profiles of q, ρ^*, β, ν^* and F_{gr} can be seen in figure 7 for the ν^* match and figure 8 for the F_{gr} match.

There is a close match for ρ^* and β for all three shots for $0.4 < x < 0.8$ (where x is the plasma radius normalised to the square root of toroidal flux). For the relevant shots the ν^* and F_{gr} matches are also close within this region. Outside this region the matches are poor. The JET q profile appears flatter than the CMOD profile, however the q_{95} value is a close match and an inversion radius of $x \approx 0.3$ suggests that the TRANSP core q profile is unreliable.

The corresponding local transport coefficients χ_{eff} normalised to Ba^2 are shown in figures 9(a) and 9(b). The upper and lower limits on the profiles of the local transport coefficients χ_{eff} were calculated using the percentage global error. Transient sawtooth activity was present in the region $0 < x < 0.4$, which makes the interpretation of transport in this region ambiguous. Data outside a radius of $x = 0.8$ are ignored to eliminate the transient effects at the pedestal. The ICRH power deposition as calculated by the PION code was more off axis in the JET discharges than in the CMOD discharge (see figures 10(a) and 10(b)), causing a more peaked temperature profile in the CMOD case. This does not seriously affect the match outside $x = 0.4$.

In the region $0.4 < x < 0.8$ the normalised local transport profiles are a close match for the ν^* match. For the F_{gr} match the profiles show a significant difference. This is consistent with the global confinement scaling; however, the lack of reliable data outside of this region does not allow one to confirm the assertion that ν^* is the more relevant dimensionless parameter in the regions outside $0.4 < x < 0.8$[19].

3.2. ν^* SCALING

The power law scaling of $B\tau_E$ with ν^* was calculated as $B_T B\tau_E \propto \nu^{*0.5\pm0.06}$. Ordinary least squares log linear regression was used with the points shown in figure 5(a). The dimensionless collisionality of the matched shots was considerably higher than is usual for JET. This may explain the strong scaling seen in this JET ν^* scan, which is similar to the dependence seen in high-collisionality scans on DIII-D where $B_T B\tau_E \propto \nu^{*0.56\pm0.06}$ [28]. This contradicts the IPB98(y,2)

scaling, $B_T B\tau_E \propto \nu^{*0.01\pm0.06}$, which is virtually independent of collisionality. It is however in agreement with the recent more sophisticated analysis of the ITER database using an errors in variables treatment[29]. Previous scans on JET [30] at lower collisionality have shown $B_T B\tau_E \propto \nu^{*0.35\pm0.04}$ and $B_T B\tau_E \propto \nu^{*0.27}$[31], which indicates that the dependence of energy confinement on collisionality is not a simple power law. Figure 11 shows the collisionality dependence for scans on several machines at different ν^* and clearly shows a trend towards increased scaling with collisionality.

SUMMARY AND CONCLUSIONS

The global confinement and local transport of a JET discharge with the dimensionless parameters ρ^*, β, ν^* matched to an Alcator-CMOD discharge was compared to the transport of a JET discharge with ρ^*, β, F_{gr} matched to the same Alcator-CMOD discharge. The normalised global energy confinement ($B_¿E$) on each machine agreed to within 1 standard deviation for the ρ^*, β, ν^* match. For the ρ^*, β, F_{gr} match the confinement differed by 5 standard deviations. Within the region $0.4 < x < 0.8$ the local normalised energy confinement is matched within error bars for the ρ^*, β, ν^* match. For the ρ^*, β, F_{gr} match the normalised energy confinement differs significantly. The JET ν^* scan, from which the matched discharges were taken showed an increase in the ν^* confinement scaling ($B_T B\tau_E \propto \nu^{*0.5\pm0.06}$) when compared to the IPB98(y,2) scaling ($B_T B\tau_E \propto \nu^{*0.01\pm0.06}$). This was consistent with previous high-collisionality ν^* scans on JET and more recent analysis of the ITER database[29].

This result supports the conclusion of previous studies [19] that ρ^*, β, ν^* is the correct set of dimensionless parameters for use in confinement scaling. Further studies are required to confirm this conclusion. The increased scaling with ν^* from this scan performed on JET, along with data from other machines, indicates that the dependence of $B_T B\tau_E$ on ν^* is not a simple power law, although the precise form of the scaling remains to be found. The apparent degradation in confinement as the Greenwald limit is approached can potentially be understood as a dependence on ν^*, which is not present in the IPB98(y,2) scaling. In order for accurate predictions to be made for ITER the dependence on collisionality needs to be more fully understood.

ACKNOWLEDGEMENTS

This work was funded jointly by the United Kingdom Engineering and Physical Sciences Research Council and by the European Communities under the contract of Association between EURATOM and UKAEA. The views and opinions expressed herein do not necessarily reflect those of the European Commission.

REFERENCES

[1]. B.B Kadomtsev. *Soviet Journal of Plasma Physics*, **1**:295, 1975.

[2]. J.W Connor and J B Taylor. *Nuclear Fusion*, **17**:1047, 1977.

[3]. C.C Petty *et al* . *Physics of Plasmas*, **5**:1695, 1998.
[4]. T.C Luce *et al* . *Nuclear Fusion*, **42**:1193, 2002.
[5]. K. Thomsen *et al* . Confinement identity experiments in asdex upgrade and jet. In *Proc. 25th EPS Conf. on Contr. Fusion and Plasma Physics*, volume 22C, page 468, Geneva, 1998. EPS.
[6]. J.P. Christiansen and J G Cordey. *Nuclear Fusion*, **38**:1757, 1998.
[7]. M. Greenwald *et al* . *Nuclear Fusion*, **28**:2199, 1988.
[8]. M. Greenwald. *Plasma Physics and Controlled Fusion*, **44**:R27, 2002.
[9]. K. Lackner. *Comments Plasma Physics and Controlled Fusion*, **13**:163, 1990.
[10]. K. Lackner. *Comments Plasma Physics and Controlled Fusion*, **15**:359, 1994.
[11]. B.B. Kadomstev. *Comments Plasma Physics and Controlled Fusion*, **13**:57, 1989.
[12]. G. Saibene *et al* . *Nuclear Fusion*, **39**:1133, 1999.
[13]. J. Stober *et al* . *Plasma Physics and Controlled Fusion*, **42**:A211, 2000.
[14]. T.H. Osborne *et al* . *Plasma Physics and Controlled Fusion*, **42**:A175, 2000.
[15]. N. Asakura *et al* . *Plasma Physics and Controlled Fusion*, **39**:1295, 1997.
[16]. J. Ongena *et al* . *Plasma Physics and Controlled Fusion*, **43**:A11–A30, 2001.
[17]. P. Dumortier *et al* . *Plasma Physics and Controlled Fusion*, **44**:1845, 2002.
[18]. O. Gruber *et al* . *Nuclear Fusion*, **41**:1369, 2001.
[19]. C.C. Petty *et al* . *Plasma Physics and Controlled Fusion*, **46**:A207, 2004.
[20]. L-G. Eriksson *et al* . *Nuclear Fusion*, **33**:1037, 1993.
[21]. D.C. McDonald *et al* . *Plasma Physics and Controlled Fusion*, **46**:A215, 2004.
[22]. G. Braithwaite *et al* . *Review of Scientific Instruments*, **60**:2825, 1989.
[23]. H. Salzmann *et al* . *Review of Scientific Instruments*, **59**:1451, 1988.
[24]. M.G von Hellerman *et al* . *Review of Scientific Instruments*, **61**:3479, 1990.
[25]. D.P. O'Brien *et al* . *Nuclear Fusion*, **32**:1351, 1992.
[26]. R.V. Budny *et al* . *Nuclear Fusion*, **35**:1497, 1995.
[27]. R.V. Budny *et al* . *Physics of Plasmas*, **7**:5038, 2000.
[28]. C.C. Petty and T C Luce. *Physics of Plasmas*, **6**:909, 2001.
[29]. J.G. Cordey *et al* . *Nuclear Fusion*, **45**:1078, 2005.
[30]. D.C. McDonald *et al* . *Particle and energy transport in dedicated dimensionless parameter scans in JET ELMy H-modes. In preparation, Plasma Physics and Controlled Fusion*, 2006.
[31]. J.G Cordey *et al* . Energy Confinement and H-mode Power Threshold Scaling in JET with ITER Dimensionless Parameters. In *Fusion Energy 1996*, volume 1, page 603, Montreal, 1997. Vienna, International Atomic Energy Agency.

Pulse No:	62663 (JET) (IO4)	62657 (JET) (I04)	1001018013 (CMOD)
Time(s)	31.38	34.68	1.26
a (m)	0.91	0.92	0.22
κ	1.68	1.67	1.67
δu	0.46	0.42	0.44
δl	0.38	0.37	0.52
W_{th} (MJ)	0.37	0.78	0.18
q_{95}	4.33	4.15	4.44
n (10^{19} m^{-3})	2.12	2.22	36.0
I (MA)	0.67	1.02	0.99
B (T)	0.95	1.38	5.5
F_{gr} ($=n\pi a^2/I$)	0.82 (– 4:4%)	0.58 (– 4:4%)	0.55 (– 5:9%)
$W_{th}/aI^2/I$ ($\propto\beta$)	0.91 (– 5:7%)	0.81 (– 5:7%)	0.83 (– 10:7%)
$(W_{th}/na^3)^{1/2}I$-1($\propto\rho*$)	0.72 (– 2:7%)	0.66 (– 2:7%)	0.69 (– 2:7%)
$n^3 a^7/W^2_{th}$ ($\propto\nu*$)	36.0 (– 10:4%)	10.0 (– 10:4%)	35.9 (– 11:2%)
$B\tau_E$	0.28 (– 11:4%)	0.69 (– 11:4%)	0.26 (– 14:6%)

Table 1. Global parameters in the ν and Greenwald JET-CMOD matches*

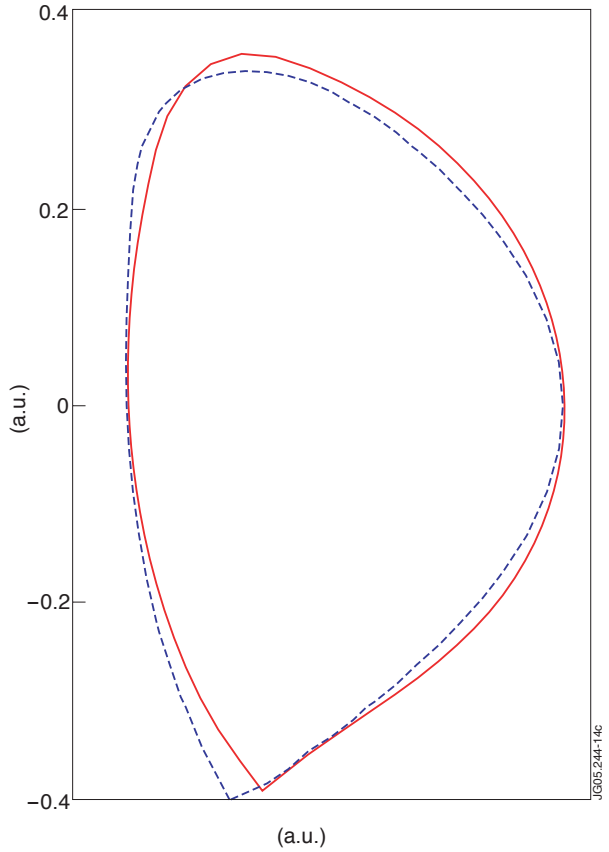

Figure 1: The last close flux surface of CMOD Pulse 1001018013 (blue/dashed) compared with the last closed flux surface of the JET ν match, Pulse No: 62663(red/solid) (calculated by EFIT) normalised to the CMOD size. The JET F_{gr} match, Pulse No: 62657 is a close match to the JET ν* match.*

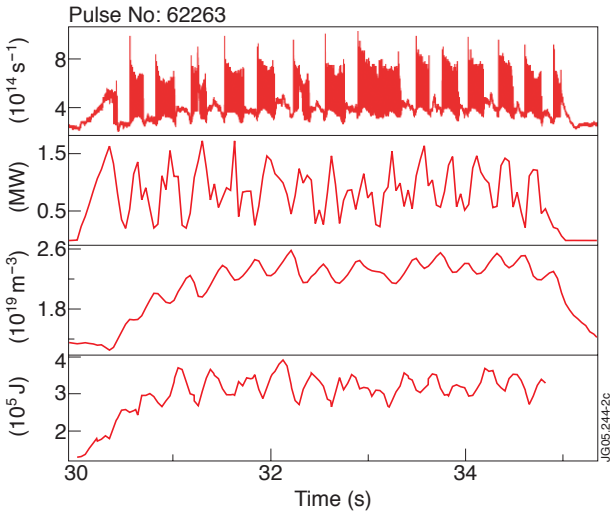

Figure 2: Time traces of the D_α signal, ICRH power, line averaged density and plasma thermal energy for the JET Pulse No: 62663, which has $\rho*$, β, $\nu*$ matched to CMOD Pulse 1001018013.

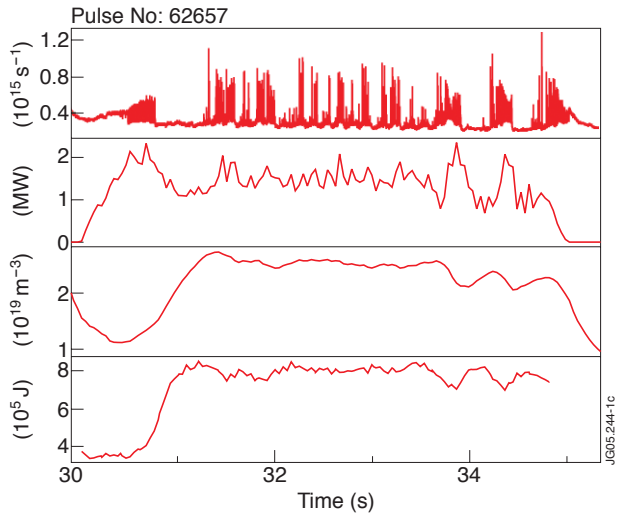

Figure 3. Time traces of the D_α signal, ICRH power, line averaged density and plasma thermal energy for the JET Pulse No: 62657, which has $\rho*$, β, F_{gr} matched to CMOD Pulse 1001018013.

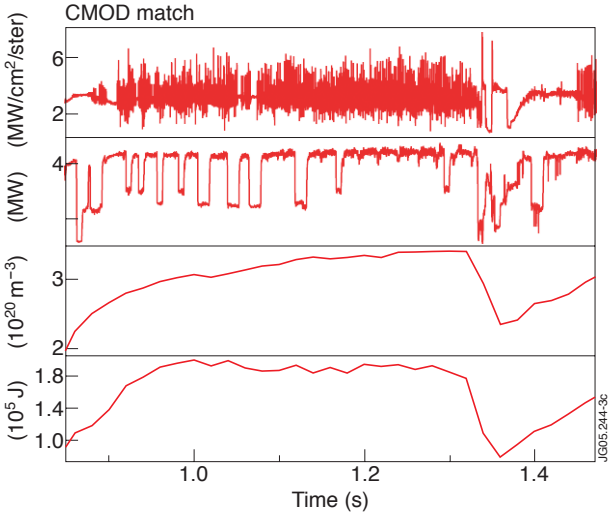

Figure 4. Time traces of the D_α signal, ICRH power, line averaged density and plasma thermal energy for the Alcator-CMOD pulse 1001018013.

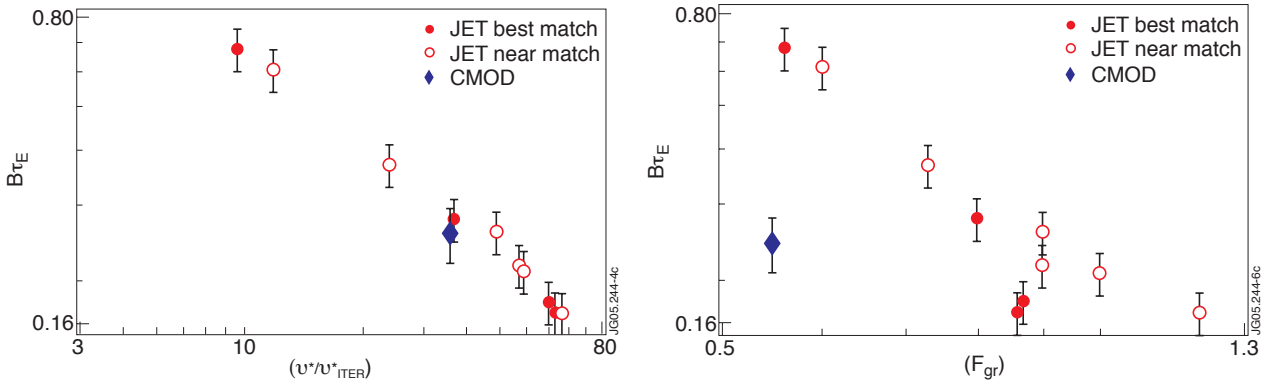

Figure 5: $B\tau_E$ versus v (a) and $B\tau_E$ versus F_{gr} (b) for discharges at JET and CMOD with matched $\rho*$, β, q and shape forming a scan in v*. The solid blue point is the CMOD data, solid red stars are the best JET v* matches and open stars are JET near matches. The degradation of $B\tau_E$ with v* can be clearly seen.*

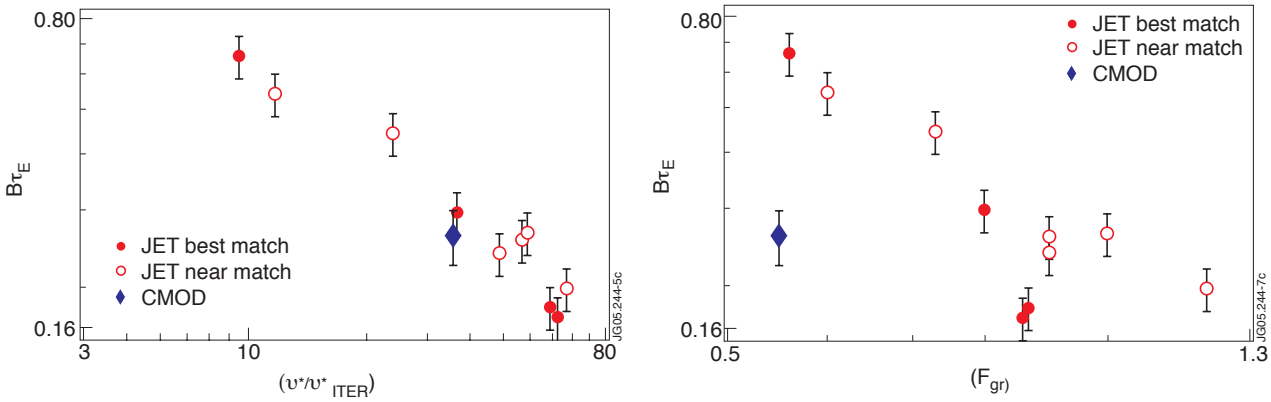

Figure 6: $B\tau_E$ versus v^*_n (a) and $B\tau_E$ versus F_{gr} (b) normalised to $\rho^{*-2.7}$ for discharges at JET and CMOD with matched $\rho*$, β, q and shape forming a scan in v. The solid blue point is the CMOD data, solid red stars are the best JET matches and open stars are JET near matches. The degradation of $B\tau_E$ with v* can be clearly seen.*

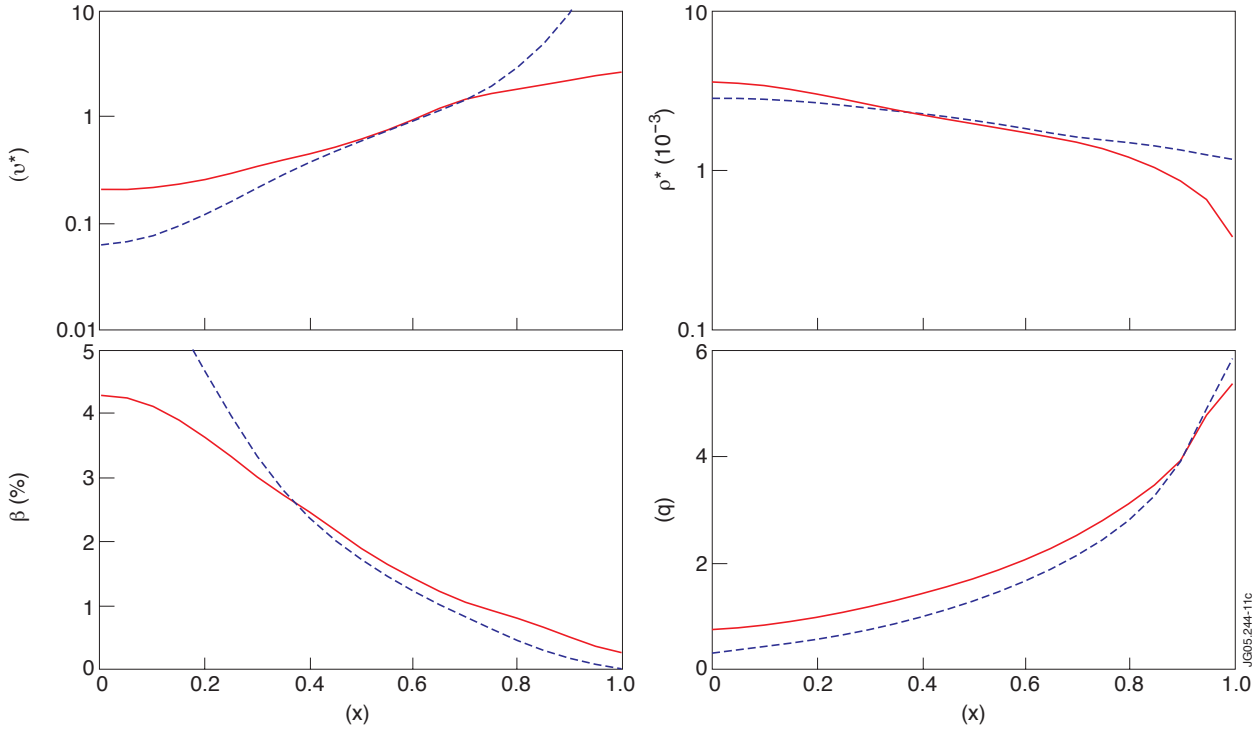

Figure 7: Profiles for the JET ν match (red/solid) and CMOD shot (blue/dashed). Starting from the top left, ν*, ρ*, β and q. The greyed area represents the estimated error calculated from the global error estimates. This does not take into account uncertainties at the edge and core.*

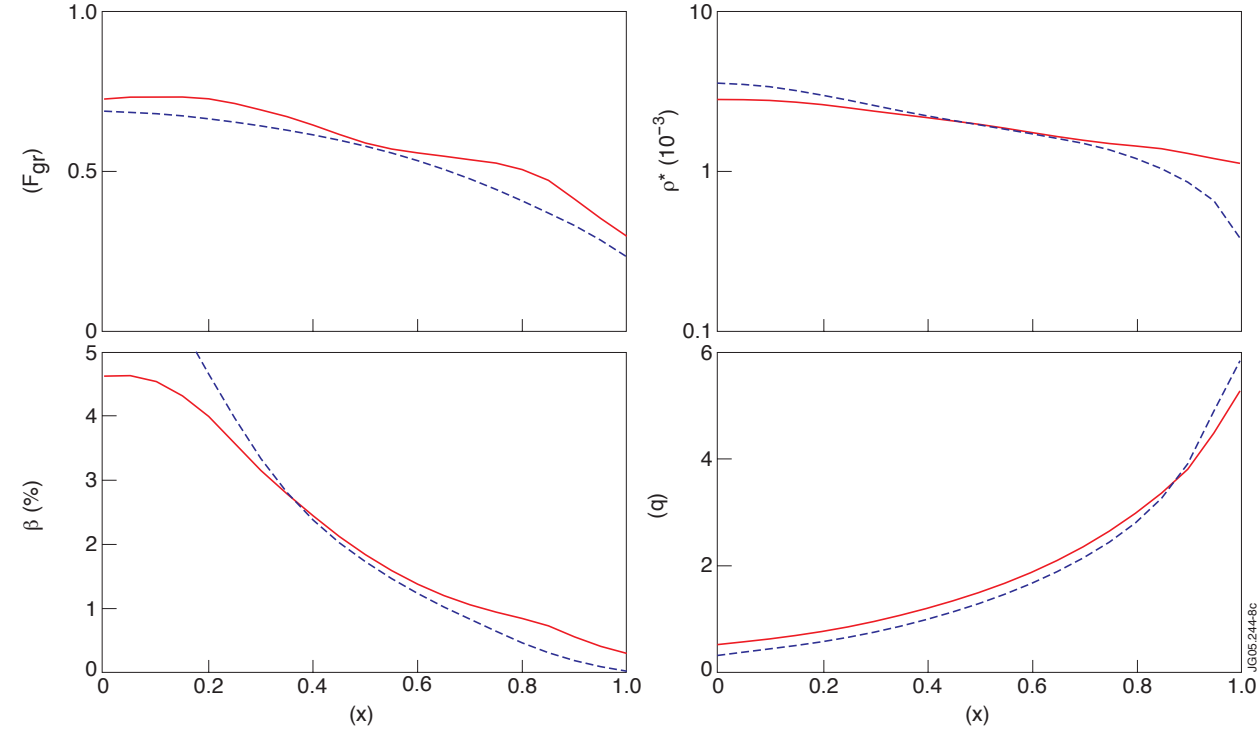

Figure 8: Profiles for the JET F_{gr} match (red/solid) and CMOD shot (blue/dashed). Starting from the top left, F_{gr}, ρ, β and q. The greyed area represents the estimated error calculated from the global error estimates. This does not take into account uncertainties at the edge and core.*

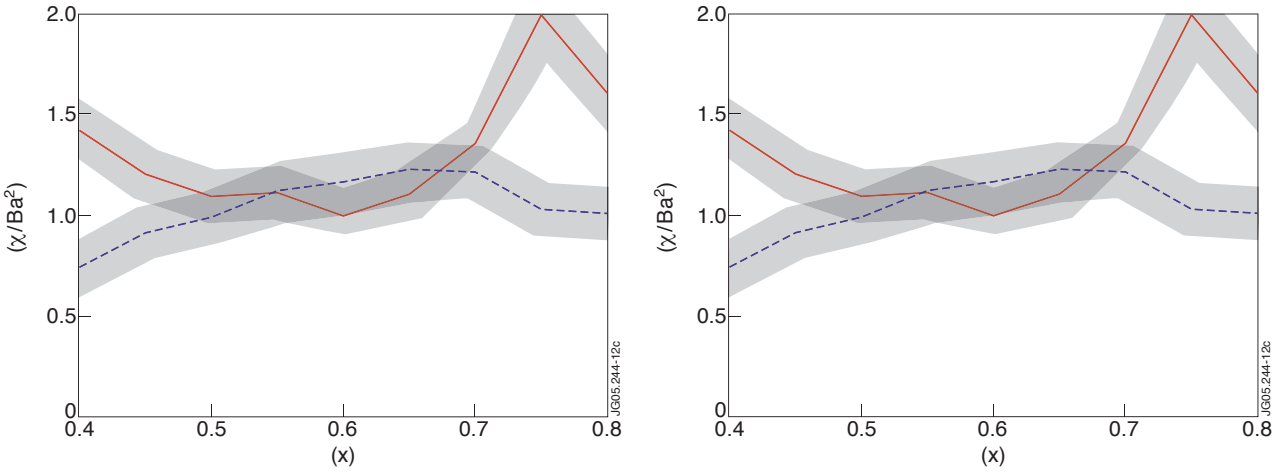

Figure 9: Profiles of the local transport coefficient χ_{eff}. The greyed area represents the estimated error calculated from the global error estimates. This does not take into account uncertainties at the edge and core. a) χ_{eff} profiles for the JET ν^* match (red/solid) and CMOD shot (blue/dashed). b) χ_{eff} profiles for the JET F_{gr} match (red/solid) and CMOD shot (blue/dashed).

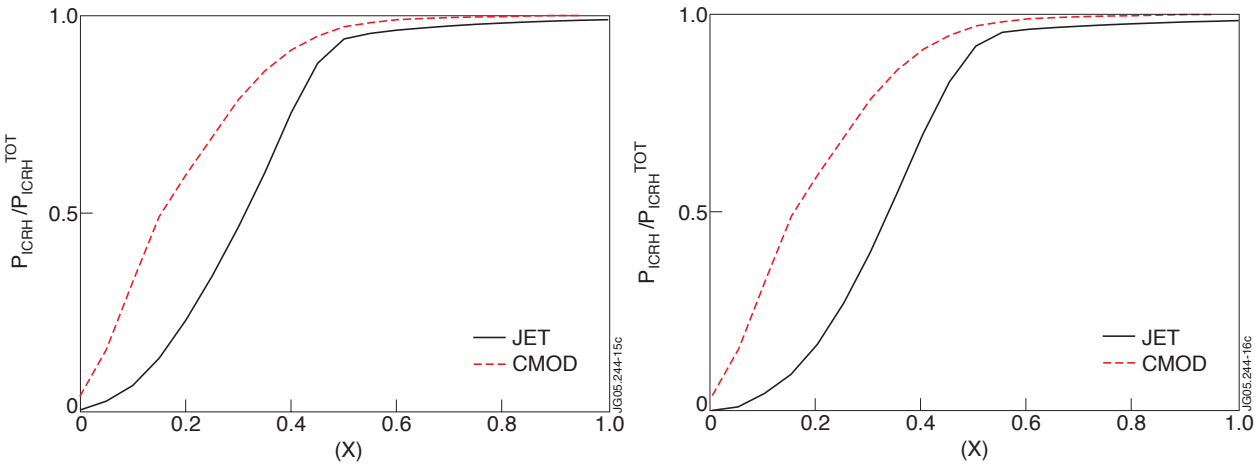

Figure 10: Normalised integrated ICRH power deposition for the JET(red/solid) ν^*(a) and F_{gr} (b) matches) and Alcator-CMOD(blue/dashed) discharge 1001018013.

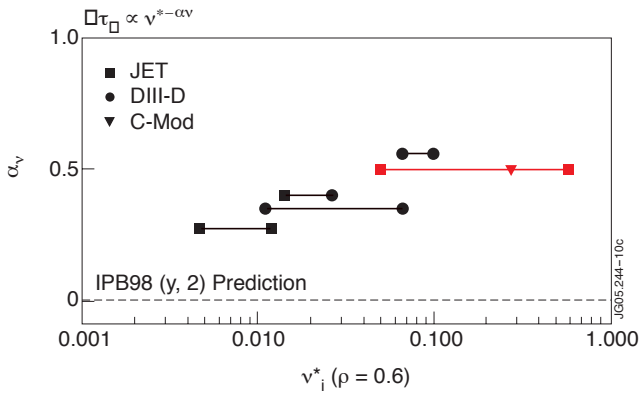

Figure 11. ν^* scalings from several different ν^* scans at fixed ν^*, β, and q performed on JET, DIII-D and Alcator-CMOD